Journal of Fluorescence, Vol. 13, No. 1, January 2003 (© 2003)

Probing the Conformational Stability of Two Different Copper Proteins: A Dynamic Fluorescence Study on Azurin and Ascorbate Oxidase

Giampiero Mei,[1] Almerinda Di Venere,[1] Eleonora Nicolai,[1] Nicola Rosato,[1] and Alessandro Finazzi Agro'[1,2]

Received

Tryptophan fluorescence is extremely useful to monitor structural conformational transitions in proteins. Denaturant-induced unfolding of azurin and ascorbate oxidase has been studied by dynamic fluorescence measurements in the frequency domain and the results have been interpreted in terms of continuous distribution of lifetimes. The data add new information on the unfolding mechanism that was previously analyzed by steady-state emission spectroscopy. In particular, the existence of multiple, parallel unfolding pathways may be envisaged and correlated, in both cases, to the two protein structures. The effect of metal depletion has been also characterized by fluorescence lifetime measurements. In the case of azurin, a monomeric protein, the data demonstrate that copper removal yields a totally different unfolding pathways with respect to the holo protein, indicating that metal ion plays a fundamental structural role in the wild type, native protein. In the case of ascorbate oxidase a dimer of 140 kDa, only minor effects have been detected by copper removal. However, the analysis of the fluorescence decay in presence of different amounts of guanidinium hydrochloride gives new important insights on the unfolding intermediates. In particular the data support the hypothesis of a partial exposure of an outer layer of dimer at intermediate denaturant concentration. This ability of dynamic fluorescence to pinpoint the presence of structural micro-heterogeneity in the unfolding pathways of proteins demonstrates the greater power of this technique compared to the most commonly used steady-state measurements.

KEY WORDS: Fluorescence dynamics; protein unfolding; lifetime distribution; azurin; ascorbate oxidase.

INTRODUCTION

The intrinsic fluorescence of proteins essentially arises from the peculiar spectroscopic properties of three amino acids: phenylalanine, tyrosine, and tryptophan. Upon excitation in the near UV, the aromatic side chains may produce a broad emission spectrum that, in the case of tryptophan, is characterized by a high quantum yield and a strong dependence on the surrounding environment. These features have transformed the protein intrinsic fluorophores in important experimental tools of molecular engineering for the investigation of structural and functional properties of proteins and enzymes. For example, whenever involved (naturally or artificially) in the active site, these aromatic aminoacids are very useful to follow the kinetics of enzymes. Radiationless energy transfer between two different aromatic aminoacids may also give

[1] Department of Experimental Medicine and Biochemical Sciences and INFM, University of Rome "Tor Vergata", Rome 00133, Italy.
[2] To whom correspondence shoud be addressed. Fax: +39-06-72596468. E-mail: mei@med.uniroma2.it

[3] ABBREVIATIONS: AAO, ascorbate oxidase; GdHCl, guanidinium hydrochloride; F110S, Phe110-Ser; I7S, Ile7-Ser; CD, circular dichroism.

1053-0509/03/0100–0033/0

information on processes taking place on a much larger structural scale, such as subunit association in oligomers or aggregation of misfolded proteins, to mention a few forefront topics of recent biochemical and biomedical investigations. Due to its higher sensitivity, tryptophan fluorescence is particularly suitable to probe the local structure of protein domains and those conformational changes that involve the surrounding protein matrix. In particular, its emission properties have been commonly used to characterize protein unfolding and refolding processes under a wide variety of denaturing agents, such as temperature, pressure, pH, SDS, urea and guanidine. Provided a great care is taken analyzing the experimental data [1], steady-state fluorescence parameters (intensity, anisotropy, spectral center of mass, etc . . .) may be used to monitor denaturation transitions in proteins by tryptophan fluorescence [2]. Quantitative information (such as the protein stabilization energy, ΔG, and its dependence on denaturant concentration, the so-called "m value") have been reported for a large number of monomeric and dimeric proteins. However, several details of the unfolding process may be lost using steady-state techniques, since measurements are time-averaged and cannot take into account a possible dynamic heterogeneity of these macromolecular systems. On the other hand, the improvement in the excitation sources and detectors has allowed to detect fluorescence lifetimes as short as 10–20 ps, revealing that protein intrinsic fluorescence decay is usually a complex multi-exponential function, a single lifetime being rarely found even in single tryptophan-containing proteins. A commonly used and alternative data analysis is based on continuously distributed sets of lifetime [3]. For frequency-domain lifetime data, fitting algorithms using both symmetric [4–6] and asymmetric-shaped gaussian [7] or lorentzian [8] distribution have been developed.

In the case of time-domain experiments, the maximum entropy [9,10] allows to recover distribution of lifetimes without any a priori knowledge of the fitting function.

We have used the first approach to study the unfolding of two different copper proteins, namely azurin and ascorbate oxidase (AAO),[3] whose native fluorescence dynamics have been previously resolved [11,12].

Azurin, a small, monomeric, electron-transfer enzyme of denitrifying bacteria, is the protein with the most blue-shifted (308 nm) fluorescence spectrum. The emission decay of its unique tryptophan residue (TRP 48) is known to be characterized by a double exponential function [13] with a long component (4.5 ns), which is quite close to the single lifetime of the apo protein (4.7 ns). Site-directed mutagenesis has demonstrated that a couple of single point mutants (Phe110-Ser and Ile7-Ser) are characterized by structural changes in the hydrophobic environment of TRP 48 [14], which affect the fluorescence dynamics of both the holo and the apo wild-type protein form [13].

AAO is instead a quite large homodimeric enzyme containing 14 tryptophan residues per subunit. This structural complexity is reflected by a quite heterogeneous fluorescence decay, which has been resolved into a double lorentzian distribution of lifetimes [12]. Multiple wavelength detection, quenching experiments and time resolved emission spectroscopy allowed to assign each distribution to a different class of tryptophans, differently exposed to the solvent.

Both azurin and AAO stability has been previously studied by circular dichroism (CD) and steady-state fluorescence in equilibrium unfolding experiments. In this paper we have extended the denaturation study to dynamic fluorescence measurements. The results give new insights on the unfolding pathways of the two proteins, reflecting those structural conformational changes, which take place during the denaturation process.

MATERIALS AND METHODS

Samples and Buffers

Recombinant wt azurin, I7S and F110S mutants were expressed, purified and prepared as previously described [15]. Apo wild-type protein was prepared according to the procedure described by Mei and coworkers [11]. The protein was dissolved in Tris-HCl 50 mM, pH 7.2.

Ascorbate oxidase from green zucchini was purchased from Roche and was dissolved in 80 mM K-phosphate buffer, pH 6.0. The apo protein was obtained as elsewhere described [16].

Equilibrium unfolding measurements were performed using stock solution of ultrapure guanidinium hydrochloride (GdHCl) purchased from United States Biochemicals, and incubating the samples at 10°C for at least 12 h in the presence of different amounts of denaturant.

Spectroscopical Assays

Dynamic fluorescence measurements were carried out using the phase-shift and demodulation technique [17] at the LASP Laboratory, Rome, Italy. The light source was a high-repetition mode-locked Nd-Yag laser. Data analysis was performed by minimizing the reduced χ^2

with a routine based on a Marquardt algorithm using the Globals Unlimited Software [18].

CD spectra were recorder using a Jasco J-710 spectropolarimeter using a 0.1 cm quartz cuvette at 20°C.

RESULTS AND DISCUSSION

Azurin

Dynamic fluorescence measurements on apo-wt azurin have been performed at different GdHCl concentration and the corresponding global lifetime distribution analysis is shown in Figure 1. The phase-shift and demodulation data of the native protein can be satisfactorily fitted according to a single lifetime, centered around 4.7 ns, as previously reported [11]. As shown in Figure 1, the unfolding process is initially characterized, between 0 and 1.6 M GdHCl, by a progressive quenching and widening of the lifetime distribution, followed by a fast decrease in the width at half maximum, which in the fully unfolded state (i.e., at 2.8 M GdHCl) is ≈ 1.0 ns.

The recovery of lifetime distributions as a function of denaturant concentration in single tryptophan containing proteins has been reported by several authors [19–22]. In most cases, a single distribution was sufficient to fit the data and results similar to those reported in Figure 1 were obtained. The increase in the distribution width upon denaturation has been generally ascribed to an enhanced heterogeneity due to the simultaneous presence of multiple molecular conformations. In other words, as the unfolding proceeds toward the fully unfolded, disordered state(s), the destruction of the compact native protein leads to a greater segmental mobility in the different part of the protein matrix. As a consequence, the intrinsic fluorescence decay, which reflects the local conformational substates probed by the tryptophan residue, becomes more complex.

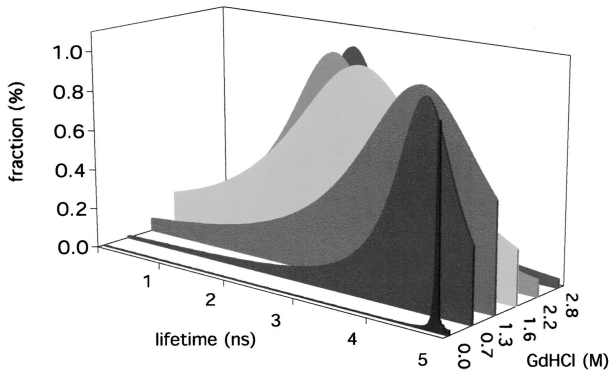

Fig. 1. Profiles of fluorescence lifetime distributions of apo wild type azurin as a function of GdHCl concentration. The curve parameters (center, c, width, w) obtained from the data analyses are: 0.0 M GdHCl, c = 4.7 ns, w = 0.04 ns; 0.7 M GdHCl, c = 4.4 ns, w = 1.0 ns; 1.3 M GdHCl, c = 4.0 ns, w = 2.1 ns; 1.6 M GdHCl, c = 2.9 ns, w = 2.6 ns; 2.2 M GdHCl, c = 2.2 ns, w = 1.7 ns; 2.8 M GdHCl, c = 2.1 ns, w = 1.2 ns.

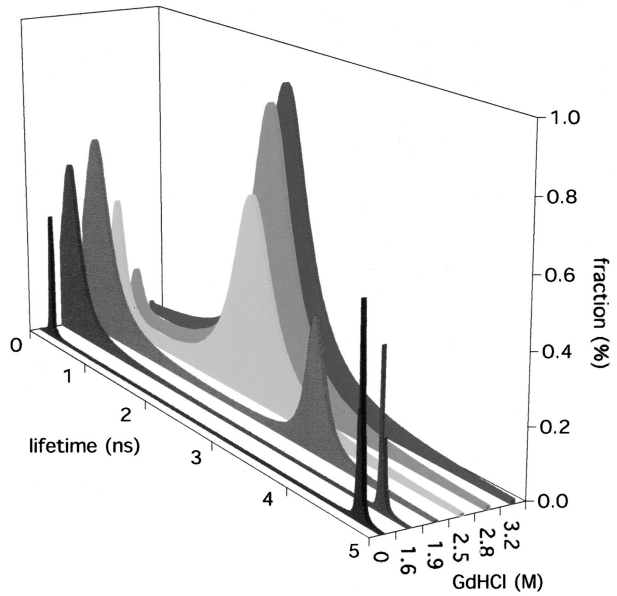

Fig. 2. Profiles of fluorescence lifetime distributions of holo wild type azurin as a function of GdHCl concentration. The curve parameters obtained from the data analyses are: 0.0 M GdHCl, c_1 = 0.2 ns, w_1 = 0.01 ns, c_2 = 4.5, ns w_2 = 0.01 ns; 1.6 M GdHCl, c_1 = 0.2 ns, w_1 = 0.35 ns, c_2 = 4.5 ns, w_2 = 0.03 ns; 1.9 M GdHCl, c_1 = 0.2 ns, w_1 = 0.49 ns, c_2 = 3.6 ns, w_2 = 0.25 ns; 2.5 M GdHCl, c_1 = 0.2 ns, w_1 = 0.25 ns, c_2 = 2.3 ns, w_2 = 0.62 ns; 2.8 M GdHCl, c_1 = 0.1 ns, w_1 = 0.20 ns, c_2 = 2.3 ns, w_2 = 0.65 ns; 3.2 M GdHCl, c_1 = 0.1 ns, w_1 = 0.01 ns, c_2 = 2.2 ns, w_2 = 0.70 ns.

This effect is complicated in holo azurin by the presence of two discrete components in the emission decay of the native protein (Fig. 2). In this case the two discrete lifetimes progressively converge to a single lifetime distribution (at 3.2 M GdHCl) almost superimposable to that obtained for the fully unfolded apo protein (Fig. 1). A comparison between Figures 1 and 2 allows to stress several differences between the unfolding pathways of the holo and apo forms which may give information also on the native protein structure. At 1.6 M GdHCl the metal depleted enzyme is known to be already at the denaturation midpoint while most of the holo azurin molecules are still in the native state [13,23]. This is well illustrated by the dynamic fluorescence results that clearly show only an increase in the width of the short component (Fig. 2). The two fluorescence lifetimes of holo azurin have been ascribed to the existence of two distinct conformations of the native enzyme, the quenching mechanism

of the short component being explained by an electron transfer or an energy transfer process between TRP 48 and the copper site [24,25]. Another explanation for the double exponential decay could be the presence of an apo-like contaminant, as suggested by the similarity of the long component to that of the apo enzyme [24]. The results of Figures 1 and 2 definitely rule out this hypothesis since at 1.3 M GdHCl a much stronger effect would be observed around 4.7 ns, as a consequence of the apo-like denaturation. On the contrary, a change in the long lifetime is produced only at ≈2.0 M GdHCl (Fig. 2), a denaturant concentration which unfolds almost 80% of the apo protein (Fig. 1) [13].

The distribution analysis reported in Figure 2 also indicates that the two holo azurin lifetimes are affected at different guanidine concentration. In particular, changes in the short component are already observed at lower denaturant concentrations, suggesting that the corresponding protein conformation is less stable than that characterized by the longer lifetime. This indicates that during the unfolding process multiple protein conformers are simultaneously present. A similar result was already suggested by time-resolved spectroscopy study [26], which demonstrates the heterogeneity of the protein population at intermediate denaturant concentration.

Site-directed mutagenesis in the protein hydrophobic core has indicated that a single aminoacid substitution in the environment of the buried tryptophan residue may greatly affect the enzyme stability [13,23]. Smaller free energies of stabilization were in fact found both in holo I7S and F110S mutants, which are changing the microenvironment of the tryptophan. The latter mutant showed rotational dynamics suggesting a looser conformation around TRP 48. The results, reported in Figures 3 and 4, seem to match fairly well these hypotheses, since at variance with holo wild type azurin, both conformations are simultaneously involved in the denaturation process. Thus, the stability of the two protein conformations are more similar in the mutants than in the native enzyme, probably due to the structural changes (such as empty or water-filled cavities) produced by site-directed mutagenesis [23]. It is worth mentioning that the largest effect is obtained for the F110S mutant at relatively low denaturant concentration (i.e., 1.2 M GdHCl), as expected from the unfolding transition curve [23].

The increase in structural heterogeneity as probed by distribution lifetime analysis is not a unique feature of azurin. For example similar findings have been reported in detail in the case of a larger dimeric enzyme that is human superoxide dismutase [27], demonstrating a general utility of dynamic fluorescence measurements in revealing the existence of structural micro heterogeneity

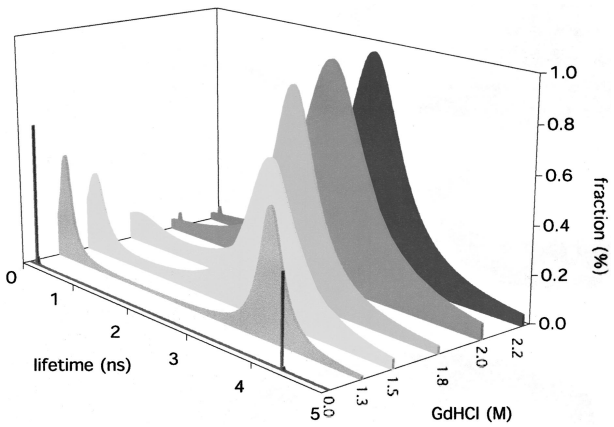

Fig. 3. Profiles of fluorescence lifetime distributions of I7S azurin as a function of GdHCl concentration. The curve parameters obtained from the data analyses are: 0.0M GdHCl, c_1 = 0.2 ns, w_1 = 0.04 ns, c_2 = 4.4 ns w_2 = 0.04 ns; 1.3 M GdHCl, c_1 = 0.2 ns, w_1 = 0.25 ns, c_2 = 3.7 ns, w_2 = 0.40 ns; 1.5 M GdHCl, c_1 = 0.2 ns, w_1 = 0.38 ns, c_2 = 3.2 ns, w_2 = 0.91 ns; 1.8 M GdHCl, c_1 = 0.2 ns, w_1 = 1.06 ns, c_2 = 2.9 ns, w_2 = 0.80 ns; 2.0 M GdHCl, c_1 = 0.2 ns, w_1 = 0.02 ns, c_2 = 2.7 ns, w_2 = 1.20 ns; 2.2 M GdHCl, c_1 = 0.2 ns, w_1 = 0.02 ns, c_2 = 2.7 ns, w_2 = 1.03 ns.

during protein unfolding. In particular lifetime measurements demonstrate the limit of steady-state technique used in equilibrium unfolding experiments. In fact, the claimed absence of intermediate species by fitting the denaturation data with a single two-state unfolding transi-

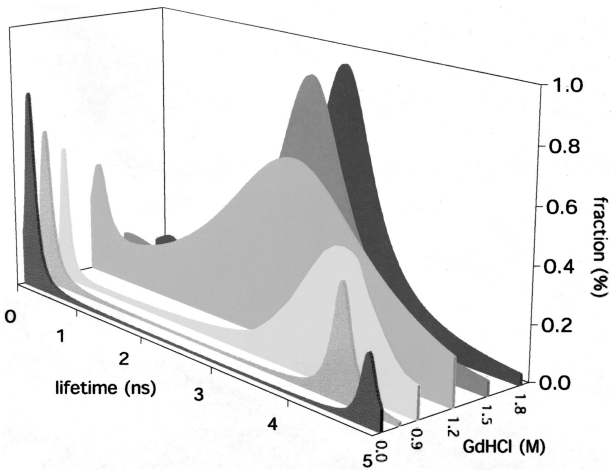

Fig. 4. Profiles of fluorescence lifetime distributions of F110S azurin as a function of GdHCl concentration. The curve parameters obtained from the data analyses are: 0.0 M GdHCl, c_1 = 0.1 ns, w_1 = 0.16 ns, c_2 = 4.8 ns, w_2 = 0.20 ns; 0.6 M GdHCl, c_1 = 0.1 ns, w_1 = 0.20 ns, c_2 = 4.3 ns, w_2 = 0.25 ns; 0.9 M GdHCl, c_1 = 0.1 ns, w_1 = 0.12 ns, c_2 = 4.1 ns, w_2 = 1.00 ns; 1.2 M GdHCl, c_1 = 0.1 ns, w_1 = 0.29 ns, c_2 = 3.0 ns, w_2 = 2.35 ns; 1.5 M GdHCl, c_1 = 0.1 ns, w_1 = 1.15 ns, c_2 = 2.7 ns, w_2 = 1.09 ns; 1.8 M GdHCl, c_1 = 0.2 ns, w_1 = 0.44 ns, c_2 = 2.7 ns w_2 = 0.92 ns.

tion, might be a misleading approximation arising from time averaging.

Ascorbate Oxidase

The unfolding of AAO is a complex process, which requires the presence of at least an intermediate species [28]. A preliminary characterization of this intermediate state has demonstrated that it lacks enzymatic activity, despite its native like tri-dimensional structure. In particular, the secondary structure content and the oligomeric assembly are almost completely retained at 1.5 M GdHCl [28] while the tertiary structure is partially lost, as revealed by ANS-binding assay. Figure 5 shows the dynamic fluorescence analysis as a function of denaturant concentration. The most relevant effect at 1.5 M GdHCl is the widening of the distribution centered around 2.5 ns, which was previously assigned to those tryptophan residues more exposed to the solvent [12]. These findings are in line with the "molten dimer" nature of the intermediate state [28]. In fact, according to this hypothesis in the first step of AAO denaturation a partial loosening of the tertiary structure occurs, leading to a progressive exposure of the outer layer of the dimer. In this context, water penetration in the protein matrix may initially affect only the less hydrophobic residues, the internal domains being still stabilized by the presence of the quaternary structure [28]. Since at 1.5 M GdHCI no enzymatic activity was recovered [28] the molten dimer state must be also characterized by the disruption of the copper binding sites. In order to ascertain whether the metal plays some role in the stabilization of the protein molecule, we have performed equilibrium unfolding experiments on the metal-depleted protein. The results, reported in Figure 6, indicate that at least a three-state process must be taken into account and that only minor changes (≈1.0 kcal/mol) occur in the first unfolding transition with respect to the holo protein unfolding process [28]. On the other hand also dynamic measurements demonstrate that the apo protein fluorescence decay is quite similar to that of the holo enzyme (data not shown). These findings rule out the possibility that the unfolding intermediate species that we addressed as a "molten dimer" is simply the metal depleted form of AAO.

Since measurements of AAO enzymatic activity have demonstrated that the protein withstands temperature changes in the range 10–50°C [29], we have also investigated its spectroscopical features as a function of temperature. Only minor changes were observed in the absorption peaks at 330 nm and 610 nm (data not shown), suggesting that the metal binding sites are not perturbed in this temperature range. Despite steady-state fluorescence was considerably quenched from 9° to 48°C, a small blue-shift (≈3 nm) in the spectral center of mass was actually observed (data not shown). Interestingly, relevant effects were instead obtained in the double lifetime distribution, as shown in Figure 7. In particular the long component undergoes the largest changes, while the width of the shorter lifetime distribution is constant between 9° and 48°C. This result is in line with the assignment of the long component to the more exposed tryptophan residues [12]. In fact, collisional quenching processes might be expected to have a larger influence on the more external

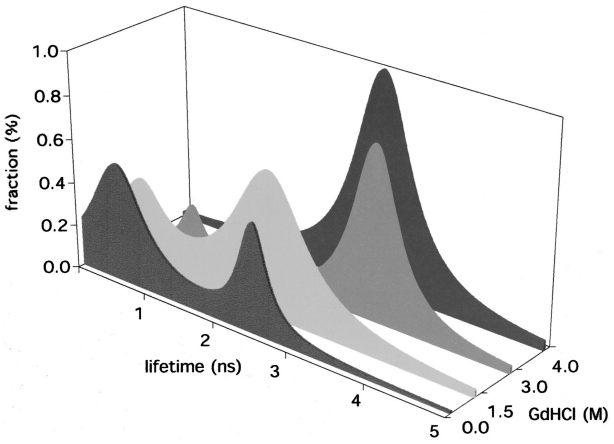

Fig. 5. Profiles of fluorescence lifetime distributions of AAO as a function of GdHCl concentration. The curve parameters obtained from the data analyses are: 0.0 M GdHCl, $c_1 = 0.6$ ns, $w_1 = 0.93$ ns, $c_2 = 2.5$ ns, $w_2 = 0.45$ ns; 1.5 M GdHCl, $c_1 = 0.5$ ns, $w_1 = 0.80$ ns, $c_2 = 2.3$ ns, $w_2 = 1.18$ ns; 3.0 M GdHCl, $c_1 = 0.7$ ns, $w_1 = 0.37$ ns, $c_2 = 3.3$ ns, $w_2 = 0.71$ ns; 4.0 M GdHCl, $c_1 = 0.5$ ns, $w_1 = 0.02$ ns, $c_2 = 2.9$ ns, $w_2 = 0.89$ ns.

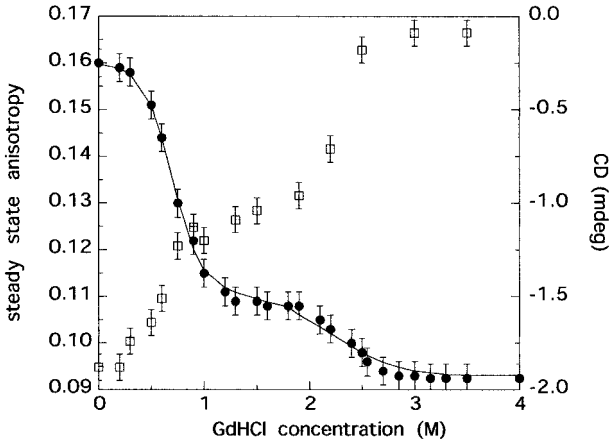

Fig. 6. Dependence of the steady state anisotropy (circles) and CD at 220 nm (squares) of apo AAO as a function of GdHCl concentration. Solid line represents the best fit obtained using a three-state denaturation model.

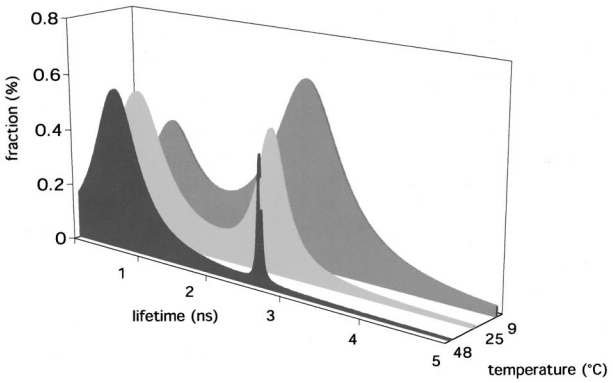

Fig. 7. Profiles of fluorescence lifetime distributions of AAO as a function of temperature. The curve parameters obtained from the data analyses are: AAO at 48°C, $c_1 = 0.6$ ns, $w_1 = 0.85$ ns, $c_2 = 2.7$ ns, $w_2 = 0.05$ ns; AAO at 25°C, $c_1 = 0.6$ ns, $w_1 = 0.93$ ns, $c_2 = 2.5$ ns, $w_2 = 0.45$ ns; AAO at 9°C, $c_1 = 0.7$ ns, $w_1 = 0.86$ ns, $c_2 = 2.6$ ns, $w_2 = 1.08$ ns.

shell of the protein structure. However, the reduced heterogeneity obtained at 48°C is only apparent, since at higher temperatures an increase in the inter-conversion of local, conformational substates might also take place. To illustrate the different effects of GdHCl and temperature on the longer lifetime distribution of AAO, we have reported in Figure 8 a possible scheme for the mechanism of the

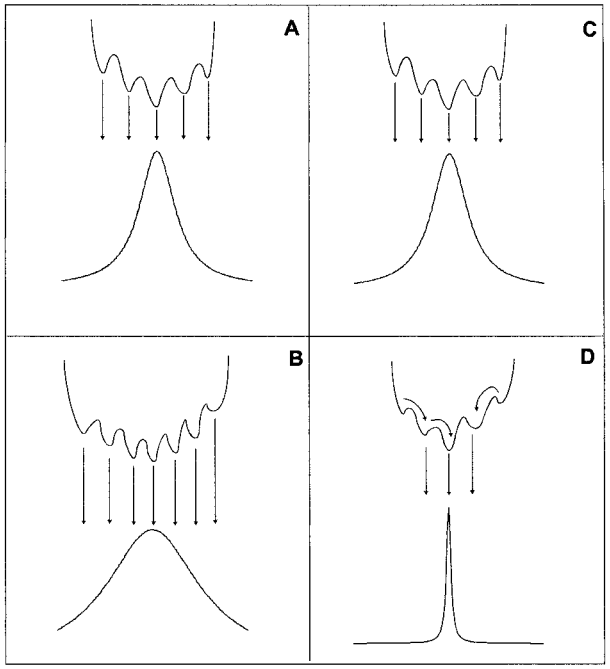

Fig. 8. Schematic diagrams of AAO excited state dynamic fluorescence emission relative to the longer lifetime distribution. Panels A and C represent the native state; panels B and D the "molten dimer" species and the protein at 48°C, respectively.

fluorescence emission decay. The two upper panels (A and C) represent the excited state ensemble of conformational substates (as probed by the tryptophanyl residues) at 20°C in absence of GdHCl. The other two panels show the widening of the distribution width due to the enhanced structural heterogeneity of the "molten dimer" state (B), or the opposite effect, due to a temperature increase (D). This simple model indicates that a correlation between the actual micro heterogeneity of the AAO protein and the temperature effects on the fluorescence decay is quite indirect and that more accurate and detailed measurements must be carried out.

In conclusion, we have shown how dynamic fluorescence measurements may give important and additional information to equilibrium unfolding experiments, even in the case of two well-studied proteins, such as azurin and AAO.

However, while the small size and the simpler structure of azurin allowed to resolve its conformational dynamics through rotational correlation measurements of the wild-type and single point mutated proteins, AAO still deserves a more accurate study. In particular a characterization of the folding dimeric intermediate by kinetic measurements and by labeling the protein with a fluorescent probe with a longer lifetime than tryptophan may help to obtain more details on the structural and functional role of the enzyme quaternary structure. These measurements are in progress in our laboratory.

REFERENCES

1. M. R. Eftink (1994) *Biophys. J.* **66**, 482–501.
2. C. N. Pace, B. A. Shirley, and J. A. Thomson (1989) In T. E. Creighton (Ed.) *Protein structure. A practical approach*, IRL Press, pp. 311–330.
3. W. R. Ware (1992) In V. Ramamurthy (Ed.) *Photochemistry in Organized and Constrained Media*, VCA, New York, pp. 563–602.
4. J. R. Alcala, E. Gratton, and F. G. Prendergast (1987) *Biophys. J.* **51**, 587–596.
5. J. R. Alcala, E. Gratton, and F. G. Prendergast (1987) *Biophys. J.* **51**, 597–604.
6. J. R. Lakowicz, H. Cherek, I. Gryczynski, N. Joshi, and M. L. Johnson (1987) *Biophys. Chem.* **28**, 35–50.
7. W. Wiczk, P. S. Eis, M. N. Fishman, M. L. Johnson, and J. R. Lakowicz (1991) *J. Fluoresc.* **1**, 273–286.
8. G. Mei, A. Di Venere, F. De Matteis, A. Lenzi, and N. Rosato (2001) *J. Fluoresc.* **11**, 319–333.
9. A. Siemiarczuk, B. D. Wagner, and W. R. Ware (1990) *J. Phys. Chem.* **94**, 1661–1666.
10. J. M. Shaver and L. B. McGown (1996) *Anal. Chem.* **68**, 9–17.
11. G. Mei, G. Gilardi, M. Venanzi, N. Rosato, G. W. Canters, and A. Finazzi Agro' (1996) *Protein Sci.* **5**, 2248–2254.
12. A. Di Venere, G. Mei, G. Gilardi, N. Rosato, F. De Matteis, R. McKay, E. Gratton, and A. Finazzi Agro' (1998) *Eur. J. Biochem.* **257**, 337–343.
13. G. Mei, N. Rosato, and A. Finazzi Agrò, (2000) In J. R. Lakowicz (Ed.) *Topics in Fluorescence Spectroscopy*, Plenum Press, New York, Vol. 6 pp. 67–81.

14. C. Hammann, A. Messerschmidt, R. Huber, H. Nar, G. Gilardi, and G. W. Canters (1996) *J. Mol. Biol.* **255**, 362–366.
15. G. Gilardi, G. Mei, N. Rosato, G. W. Canters, and A. Finazzi Agro' (1994) *Biochemistry* **33**, 1425–1432.
16. L. Morpurgo, I. Savini, B. Mondovi', and L. Avigliano (1987) *J. Inorg. Biochem.* **29**, 25–31.
17. E. Gratton and M. Limkeman (1983) *Biophys. J.* **44**, 315–324.
18. J. M. Beechem and E. Gratton (1988) *Proc. SPIE-Int. Soc. Opt. Eng.* **909**, 70–81.
19. E. Bismuto, E. Gratton, and G. Irace (1988) *Biochemistry* **27**, 2132–2136.
20. G. Mei, N. Rosato, N. Silva Jr, R. Rusch, E. Gratton, I. Savini, and A. Finazzi Agro' (1992) *Biochemistry* **31**, 7224–7230.
21. S. T. Ferreira, L. Stella, and E. Gratton (1994) *Biophys. J.* **66**, 1185–1196.
22. M. Lasagna, E. Gratton, D. M. Jameson, and J. E. Brunet (1999) *Biophys. J.* **76**, 443–450.
23. G. Mei, A. Di Venere, F. Malvezzi Campeggi, G. Gilardi, N. Rosato, F. De Matteis, and A. Finazzi Agro' (1999) *Eur. J. Biochem.* **265**, 619–626.
24. J. W. Petrich, J. W. Longworth, and G. R. Fleming (1987) *Biochemistry* **26**, 2711–2722.
25. J. E. Hansen, J. M. Longworth, and G. R. Fleming (1990) *Biochemistry* **29**, 7329–7338.
26. P. Guptasarma (1996) *Biophys. Chem.* **65**, 221–228.
27. N. Silva, E. Gratton, G. Mei, N. Rosato, R. Rusch, R. and A. Finazzi Agro' (1993) *Biophysical Chem.* **48**, 171–182.
28. G. Mei, A. Di Venere, M. Buganza, P. Vecchini, N. Rosato, and A. Finazzi Agro' (1997) *Biochemistry* **36**, 10917–10922.
29. M. Maccarrone, G. D'Andrea, M. L. Salucci, L. Avigliano, and A. Finazzi Agro' (1993) *Photochemistry* **32**, 795–798.